

Nuclear Dependence of the Transverse Single-Spin Asymmetry in the Production of Charged Hadrons at Forward Rapidity in Polarized $p+p$, $p+Al$, and $p+Au$ Collisions at $\sqrt{s_{NN}}=200$ GeV

C. Aidala,⁴⁰ Y. Akiba,^{52,53,†} M. Alfred,²³ V. Andrieux,⁴⁰ N. Apadula,²⁸ H. Asano,^{33,52} B. Azmoun,⁷ V. Babintsev,²⁴ N. S. Bandara,³⁹ K. N. Barish,⁸ S. Bathe,^{5,53} A. Bazilevsky,⁷ M. Beaumier,⁸ R. Belmont,^{12,46} A. Berdnikov,⁵⁵ Y. Berdnikov,⁵⁵ D. S. Blau,^{32,43} J. S. Bok,⁴⁵ M. L. Brooks,³⁵ J. Bryslawskyj,^{5,8} V. Bumazhnov,²⁴ S. Campbell,¹³ V. Canoa Roman,⁵⁸ R. Cervantes,⁵⁸ C. Y. Chi,¹³ M. Chiu,⁷ I. J. Choi,²⁵ J. B. Choi,^{10,*} Z. Citron,⁶³ M. Connors,^{21,53} N. Cronin,⁵⁸ M. Csanád,¹⁶ T. Csörgő,^{17,64} T. W. Danley,⁴⁷ M. S. Daugherty,¹ G. David,^{7,15,58} K. DeBlasio,⁴⁴ K. Dehmelt,⁵⁸ A. Denisov,²⁴ A. Deshpande,^{7,53,58} E. J. Desmond,⁷ A. Dion,⁵⁸ D. Dixit,⁵⁸ J. H. Do,⁶⁵ A. Drees,⁵⁸ K. A. Drees,⁶ J. M. Durham,³⁵ A. Durum,²⁴ A. Enokizono,^{52,54} H. En'yo,⁵² S. Esumi,⁶¹ B. Fadem,⁴¹ W. Fan,⁵⁸ N. Feege,⁵⁸ D. E. Fields,⁴⁴ M. Finger,⁹ M. Finger, Jr.,⁹ S. L. Fokin,³² J. E. Frantz,⁴⁷ A. Franz,⁷ A. D. Frawley,²⁰ Y. Fukuda,⁶¹ C. Gal,⁵⁸ P. Gallus,¹⁴ E. A. Gamez,⁴⁰ P. Garg,^{3,58} H. Ge,⁵⁸ F. Giordano,²⁵ Y. Goto,^{52,53} N. Grau,² S. V. Greene,⁶² M. Grosse Perdekamp,²⁵ T. Gunji,¹¹ H. Guragain,²¹ T. Hachiya,^{42,52,53} J. S. Haggerty,⁷ K. I. Hahn,¹⁸ H. Hamagaki,¹¹ H. F. Hamilton,¹ S. Y. Han,^{18,52} J. Hanks,⁵⁸ S. Hasegawa,²⁹ T. O. S. Haseler,²¹ X. He,²¹ T. K. Hemmick,⁵⁸ J. C. Hill,²⁸ K. Hill,¹² A. Hodges,²¹ R. S. Hollis,⁸ K. Homma,²² B. Hong,³¹ T. Hoshino,²² N. Hotvedt,²⁸ J. Huang,⁷ S. Huang,⁶² K. Imai,²⁹ M. Inaba,⁶¹ A. Iordanova,⁸ D. Isenhower,¹ S. Ishimaru,⁴² D. Ivanishchev,⁵¹ B. V. Jacak,⁵⁸ M. Jezghani,²¹ Z. Ji,⁵⁸ X. Jiang,³⁵ B. M. Johnson,^{7,21} D. Jouan,⁴⁹ D. S. Jumper,²⁵ J. H. Kang,⁶⁵ D. Kapukchyan,⁸ S. Karthas,⁵⁸ D. Kawall,³⁹ A. V. Kazantsev,³² V. Khachatryan,⁵⁸ A. Khanzadeev,⁵¹ C. Kim,^{8,31} E.-J. Kim,¹⁰ M. Kim,^{52,56} D. Kincses,¹⁶ E. Kistenev,⁷ J. Klatsky,²⁰ P. Kline,⁵⁸ T. Koblesky,¹² D. Kotov,^{51,55} S. Kudo,⁶¹ B. Kurgiyis,¹⁶ K. Kurita,⁵⁴ Y. Kwon,⁶⁵ J. G. Lajoie,²⁸ A. Lebedev,²⁸ S. Lee,⁶⁵ S. H. Lee,^{28,58} M. J. Leitch,³⁵ Y. H. Leung,⁵⁸ N. A. Lewis,⁴⁰ X. Li,³⁵ S. H. Lim,^{35,65} M. X. Liu,³⁵ V.-R. Loggins,²⁵ S. Lökös,^{16,17} K. Lovasz,¹⁵ D. Lynch,⁷ T. Majoros,¹⁵ Y. I. Makdisi,⁶ M. Makek,⁶⁶ V. I. Manko,³² E. Mannel,⁷ M. McCumber,³⁵ P. L. McGaughey,³⁵ D. McGlinchey,^{12,35} C. McKinney,²⁵ M. Mendoza,⁸ W. J. Metzger,¹⁷ A. C. Mignerey,³⁸ A. Milov,⁶³ D. K. Mishra,⁴ J. T. Mitchell,⁷ Iu. Mitrakov,⁵⁵ G. Mitsuka,^{30,52,53} S. Miyasaka,^{52,60} S. Mizuno,^{52,61} P. Montuenga,²⁵ T. Moon,⁶⁵ D. P. Morrison,⁷ S. I. Morrow,⁶² T. Murakami,^{33,52} J. Murata,^{52,54} K. Nagai,⁶⁰ K. Nagashima,^{22,52} T. Nagashima,⁵⁴ J. L. Nagle,¹² M. I. Nagy,¹⁶ I. Nakagawa,^{52,53} K. Nakano,^{52,60} C. Nattrass,⁵⁹ S. Nelson,¹⁹ T. Niida,⁶¹ R. Nishitani,⁴² R. Nouicer,^{7,53} T. Novák,^{17,64} N. Novitzky,⁵⁸ A. S. Nyanin,³² E. O'Brien,⁷ C. A. Ogilvie,²⁸ J. D. Orjuela Koop,¹² J. D. Osborn,⁴⁰ A. Oskarsson,³⁶ G. J. Ottino,⁴⁴ K. Ozawa,^{30,61} V. Pantuev,²⁶ V. Papavassiliou,⁴⁵ J. S. Park,⁵⁶ S. Park,^{52,56,58} S. F. Pate,⁴⁵ M. Patel,²⁸ W. Peng,⁶² D. V. Perepelitsa,^{7,12} G. D. N. Perera,⁴⁵ D. Yu. Peressouko,³² C. E. PerezLara,⁵⁸ J. Perry,²⁸ R. Petti,⁷ M. Phipps,^{7,25} C. Pinkenburg,⁷ R. P. Pisani,⁷ A. Pun,⁴⁷ M. L. Purschke,⁷ P. V. Radzevich,⁵⁵ K. F. Read,^{48,59} D. Reynolds,⁵⁷ V. Riabov,^{43,51} Y. Riabov,^{51,55} D. Richford,⁵ T. Rinn,²⁸ S. D. Rolnick,⁸ M. Rosati,²⁸ Z. Rowan,⁵ J. Runchey,²⁸ A. S. Safonov,⁵⁵ T. Sakaguchi,⁷ H. Sako,²⁹ V. Samsonov,^{43,51} M. Sarsour,²¹ S. Sato,²⁹ C. Y. Scarlett,¹⁹ B. Schaefer,⁶² B. K. Schmoll,⁵⁹ K. Sedgwick,⁸ R. Seidl,^{52,53} A. Sen,^{28,59} R. Seto,⁸ A. Sexton,³⁸ D. Sharma,⁵⁸ I. Shein,²⁴ T.-A. Shibata,^{52,60} K. Shigaki,²² M. Shimomura,^{28,42} T. Shioya,⁶¹ P. Shukla,⁴ A. Sickles,²⁵ C. L. Silva,³⁵ D. Silvermyr,³⁶ B. K. Singh,³ C. P. Singh,³ V. Singh,³ M. J. Skoby,⁴⁰ M. Slunečka,⁹ K. L. Smith,²⁰ M. Snowball,³⁵ R. A. Soltz,³⁴ W. E. Sondheim,³⁵ S. P. Sorensen,⁵⁹ I. V. Sourikova,⁷ P. W. Stankus,⁴⁸ S. P. Stoll,⁷ T. Sugitate,²² A. Sukhanov,⁷ T. Sumita,⁵² J. Sun,⁵⁸ Z. Sun,¹⁵ S. Suzuki,⁴² J. Sziklai,⁶⁴ K. Tanida,^{29,53,56} M. J. Tannenbaum,⁷ S. Tarafdar,^{62,63} A. Taranenko,⁴³ G. Tarnai,¹⁵ R. Tieulent,^{21,37} A. Timilsina,²⁸ T. Todoroki,^{53,61} M. Tomášek,¹⁴ C. L. Towell,¹ R. S. Towell,¹ I. Tseruya,⁶³ Y. Ueda,²² B. Ujvari,¹⁵ H. W. van Hecke,³⁵ J. Velkovska,⁶² M. Virius,¹⁴ V. Vrba,^{14,27} N. Vukman,⁶⁶ X. R. Wang,^{45,53} Z. Wang,⁵ Y. S. Watanabe,¹¹ C. P. Wong,²¹ C. L. Woody,⁷ C. Xu,⁴⁵ Q. Xu,⁶² L. Xue,²¹ S. Yalcin,⁵⁸ Y. L. Yamaguchi,^{53,58} H. Yamamoto,⁶¹ A. Yanovich,²⁴ J. H. Yoo,^{31,53} I. Yoon,⁵⁶ H. Yu,^{45,50} I. E. Yushmanov,³² W. A. Zajc,¹³ A. Zelenski,⁶ Y. Zhai,²⁸ S. Zharko,⁵⁵ and L. Zou⁸

(PHENIX Collaboration)

¹Abilene Christian University, Abilene, Texas 79699, USA²Department of Physics, Augustana University, Sioux Falls, South Dakota 57197, USA³Department of Physics, Banaras Hindu University, Varanasi 221005, India⁴Bhabha Atomic Research Centre, Bombay 400 085, India⁵Baruch College, City University of New York, New York, New York 10010, USA

- ⁶Collider-Accelerator Department, Brookhaven National Laboratory, Upton, New York 11973-5000, USA
- ⁷Physics Department, Brookhaven National Laboratory, Upton, New York 11973-5000, USA
- ⁸University of California-Riverside, Riverside, California 92521, USA
- ⁹Charles University, Ovocný trh 5, Praha 1, 116 36, Prague, Czech Republic
- ¹⁰Chonbuk National University, Jeonju, 561-756, Korea
- ¹¹Center for Nuclear Study, Graduate School of Science, University of Tokyo, 7-3-1 Hongo, Bunkyo, Tokyo 113-0033, Japan
- ¹²University of Colorado, Boulder, Colorado 80309, USA
- ¹³Columbia University, New York, New York 10027 and Nevis Laboratories, Irvington, New York 10533, USA
- ¹⁴Czech Technical University, Zikova 4, 166 36 Prague 6, Czech Republic
- ¹⁵Debrecen University, H-4010 Debrecen, Egyetem tér 1, Hungary
- ¹⁶ELTE, Eötvös Loránd University, H-1117 Budapest, Pázmány P. s. 1/A, Hungary
- ¹⁷Eszterházy Károly University, Károly Róbert Campus, H-3200 Gyöngyös, Mátrai út 36, Hungary
- ¹⁸Ewha Womans University, Seoul 120-750, Korea
- ¹⁹Florida A&M University, Tallahassee, Florida 32307, USA
- ²⁰Florida State University, Tallahassee, Florida 32306, USA
- ²¹Georgia State University, Atlanta, Georgia 30303, USA
- ²²Hiroshima University, Kagamiyama, Higashi-Hiroshima 739-8526, Japan
- ²³Department of Physics and Astronomy, Howard University, Washington, D.C. 20059, USA
- ²⁴IHEP Protvino, State Research Center of Russian Federation, Institute for High Energy Physics, Protvino, 142281, Russia
- ²⁵University of Illinois at Urbana-Champaign, Urbana, Illinois 61801, USA
- ²⁶Institute for Nuclear Research of the Russian Academy of Sciences, prospekt 60-letiya Oktyabrya 7a, Moscow 117312, Russia
- ²⁷Institute of Physics, Academy of Sciences of the Czech Republic, Na Slovance 2, 182 21 Prague 8, Czech Republic
- ²⁸Iowa State University, Ames, Iowa 50011, USA
- ²⁹Advanced Science Research Center, Japan Atomic Energy Agency, 2-4 Shirakata Shirane, Tokai-mura, Naka-gun, Ibaraki-ken 319-1195, Japan
- ³⁰KEK, High Energy Accelerator Research Organization, Tsukuba, Ibaraki 305-0801, Japan
- ³¹Korea University, Seoul 02841, Korea
- ³²National Research Center “Kurchatov Institute”, Moscow, 123098 Russia
- ³³Kyoto University, Kyoto 606-8502, Japan
- ³⁴Lawrence Livermore National Laboratory, Livermore, California 94550, USA
- ³⁵Los Alamos National Laboratory, Los Alamos, New Mexico 87545, USA
- ³⁶Department of Physics, Lund University, Box 118, SE-221 00 Lund, Sweden
- ³⁷IPNL, CNRS/IN2P3, Univ Lyon, Universit Lyon 1, F-69622, Villeurbanne, France
- ³⁸University of Maryland, College Park, Maryland 20742, USA
- ³⁹Department of Physics, University of Massachusetts, Amherst, Massachusetts 01003-9337, USA
- ⁴⁰Department of Physics, University of Michigan, Ann Arbor, Michigan 48109-1040, USA
- ⁴¹Muhlenberg College, Allentown, Pennsylvania 18104-5586, USA
- ⁴²Nara Women’s University, Kita-uoya Nishi-machi Nara 630-8506, Japan
- ⁴³National Research Nuclear University, MEPhI, Moscow Engineering Physics Institute, Moscow, 115409, Russia
- ⁴⁴University of New Mexico, Albuquerque, New Mexico 87131, USA
- ⁴⁵New Mexico State University, Las Cruces, New Mexico 88003, USA
- ⁴⁶Physics and Astronomy Department, University of North Carolina at Greensboro, Greensboro, North Carolina 27412, USA
- ⁴⁷Department of Physics and Astronomy, Ohio University, Athens, Ohio 45701, USA
- ⁴⁸Oak Ridge National Laboratory, Oak Ridge, Tennessee 37831, USA
- ⁴⁹IPN-Orsay, Univ. Paris-Sud, CNRS/IN2P3, Université Paris-Saclay, BP1, F-91406, Orsay, France
- ⁵⁰Peking University, Beijing 100871, People’s Republic of China
- ⁵¹PNPI, Petersburg Nuclear Physics Institute, Gatchina, Leningrad region, 188300, Russia
- ⁵²RIKEN Nishina Center for Accelerator-Based Science, Wako, Saitama 351-0198, Japan
- ⁵³RIKEN BNL Research Center, Brookhaven National Laboratory, Upton, New York 11973-5000, USA
- ⁵⁴Physics Department, Rikkyo University, 3-34-1 Nishi-Ikebukuro, Toshima, Tokyo 171-8501, Japan
- ⁵⁵Saint Petersburg State Polytechnic University, St. Petersburg, 195251 Russia
- ⁵⁶Department of Physics and Astronomy, Seoul National University, Seoul 151-742, Korea
- ⁵⁷Chemistry Department, Stony Brook University, SUNY, Stony Brook, New York 11794-3400, USA
- ⁵⁸Department of Physics and Astronomy, Stony Brook University, SUNY, Stony Brook, New York 11794-3800, USA
- ⁵⁹University of Tennessee, Knoxville, Tennessee 37996, USA
- ⁶⁰Department of Physics, Tokyo Institute of Technology, Oh-okayama, Meguro, Tokyo 152-8551, Japan
- ⁶¹Tomonaga Center for the History of the Universe, University of Tsukuba, Tsukuba, Ibaraki 305, Japan
- ⁶²Vanderbilt University, Nashville, Tennessee 37235, USA
- ⁶³Weizmann Institute, Rehovot 76100, Israel

⁶⁴*Institute for Particle and Nuclear Physics, Wigner Research Centre for Physics, Hungarian Academy of Sciences (Wigner RCP, RMKI) H-1525 Budapest 114, P.O. Box 49, Budapest, Hungary*

⁶⁵*Yonsei University, IPAP, Seoul 120-749, Korea*

⁶⁶*Department of Physics, Faculty of Science, University of Zagreb, Bijenička c. 32 HR-10002 Zagreb, Croatia*



(Received 18 March 2019; revised manuscript received 2 July 2019; published 17 September 2019)

We report on the nuclear dependence of transverse single-spin asymmetries (TSSAs) in the production of positively charged hadrons in polarized $p^\uparrow + p$, $p^\uparrow + \text{Al}$, and $p^\uparrow + \text{Au}$ collisions at $\sqrt{s_{NN}} = 200$ GeV. The measurements have been performed at forward rapidity ($1.4 < \eta < 2.4$) over the range of transverse momentum ($1.8 < p_T < 7.0$ GeV/ c) and Feynman x ($0.1 < x_F < 0.2$). We observed positive asymmetries for positively charged hadrons in $p^\uparrow + p$ collisions, and significantly reduced asymmetries in $p^\uparrow + A$ collisions. These results reveal a nuclear dependence of TSSAs for charged-hadron production in a regime where perturbative techniques are applicable. These results provide new opportunities to use $p^\uparrow + A$ collisions as a tool to investigate the rich phenomena behind TSSAs in hadronic collisions and to use TSSAs as a new handle in studying small-system collisions.

DOI: [10.1103/PhysRevLett.123.122001](https://doi.org/10.1103/PhysRevLett.123.122001)

Understanding the transverse-single-spin asymmetries (TSSAs) that describe the azimuthal-angular dependence of particle production relative to the transverse-spin direction of the polarized proton in the reaction $p^\uparrow + p \rightarrow h + X$ has been a long-standing puzzle. The first observations in pion production at large Feynman x (x_F) [1] showed measured TSSAs that were considerably larger than early theoretical predictions (in the collinear leading twist approach) [2]. Surprisingly large measured TSSAs continued to persist in hadronic collisions at high energies up to $\sqrt{s} = 500$ GeV [3–14]. To explain these large TSSAs, two approaches were proposed within perturbative quantum chromodynamics (pQCD). One approach is called transverse-momentum-dependent factorization, in which TSSAs are generated by correlations between the nucleons transverse spin direction and the transverse momentum of a parton in the polarized nucleon (Sivers effect [15,16]), and from the fragmentation of a transversely polarized parton into a final-state hadron (Collins effect [17]). Another approach, directly applicable to single-hadron production (with $p_T \gg \Lambda_{\text{QCD}}$) presented in this Letter is the twist-3, collinear-factorization framework [18]. The full description of TSSAs in $p^\uparrow + p \rightarrow h + X$ in the twist-3 collinear factorization includes twist-3 functions from the polarized proton, the unpolarized proton, and the parton fragmentation into final-state hadrons. The twist-3 functions describe quark-gluon-quark correlations and trigluon correlations in the polarized proton and have been studied in detail [19–27]. Recently, calculations of the twist-3 contribution from parton fragmentation have been carried out and have

shown this to be an important mechanism for understanding TSSA measurements [28–30].

The Relativistic Heavy Ion Collider (RHIC) is a unique facility that can accelerate polarized protons and collide them with other (polarized) protons or nuclei [31]. The extension of TSSA measurements to $p^\uparrow + A$ collisions not only gives us a crucial tool for understanding the nature of TSSAs, but also provides a new handle for studying $p + A$ collisions and the parton dynamics inside nuclei, where many emergent effects remain to be understood. These include the so-called ‘‘Cronin’’ effect, an enhancement in the inclusive hadron p_T spectrum with respect to $p + p$ collisions at moderate p_T of approximately $2 < p_T < 6$ GeV/ c that is proposed to be due to multiple scattering effects in the nuclear medium and modified hadronization mechanism [32–35]. Another exciting observation is that the collective behavior across large pseudorapidity ranges in high multiplicity $p + A$ collisions may indicate quark-gluon-plasma formation [36–38]. Furthermore, when hadron production is measured in the proton-going direction, the properties of nuclear gluons in the small- x region can be probed, where x is the fraction of the proton’s longitudinal momentum carried by the parton. The dynamics of gluons in the small- x regime, where the gluon density is predicted to increase drastically, can be described by the color-glass condensate (CGC) formalism [39] at the saturation scale Q_s , where $Q_s^2 \propto A^{1/3}$ for the target nucleus [40,41]. In recent years, substantial attention has been given to an interplay between small- x physics and spin physics by studying TSSAs in transversely polarized proton and ion collisions ($p^\uparrow + A$) and gluon saturation effects in a nucleus are taken into account for various calculations of TSSAs in $p^\uparrow + A$ collisions [40–51]. An A dependence of TSSAs can arise from the A dependence of Q_s when the probe is at or below Q_s , while TSSAs are expected to be A independent at higher scales [42,43,49–51]. Therefore, experimental data

Published by the American Physical Society under the terms of the Creative Commons Attribution 4.0 International license. Further distribution of this work must maintain attribution to the author(s) and the published article’s title, journal citation, and DOI. Funded by SCOAP³.

on hadron TSSAs measured in $p + A$ collisions with varying A size will provide valuable information testing these models and bring new insights in understanding the dynamics of the $p + A$ collisions.

We report here on the observation of a nuclear dependence of TSSAs of positively charged-hadron production at forward rapidity ($0.1 < x_F < 0.2$ and $1.4 < \eta < 2.4$, probing $0.004 \lesssim x \lesssim 0.1$ in the nuclei) in collisions between transversely polarized protons and unpolarized protons or nuclei, $p^\uparrow + p$, $p^\uparrow + \text{Al}$, $p^\uparrow + \text{Au}$ at $\sqrt{s_{NN}} = 200$ GeV measured with the PHENIX detector. The positively charged hadron is preferred in the nuclear-dependence measurement because the significance of TSSAs for negatively charged hadrons will be reduced by the partial cancellation of the asymmetry due to opposite signs of TSSAs for π^- and K^- in $p^\uparrow + p$ collisions [8,10]. In this measurement, we follow the convention to quantify TSSAs as A_N , where A_N is the modulation of the azimuthal angle of the hadron (ϕ_h) relative to the azimuthal angle of the transverse spin of the proton (ϕ_{pol}), i.e., hadron-production cross section $\sigma \propto 1 + A_N \sin(\phi_{\text{pol}} - \phi_h)$.

The data from transversely polarized $p^\uparrow + p$, $p^\uparrow + \text{Al}$, and $p^\uparrow + \text{Au}$ collisions at $\sqrt{s_{NN}} = 200$ GeV were collected with the PHENIX detector during the RHIC 2015 running period. Proton beams were polarized vertically with respect to the beam direction with an average polarization of 58% (clockwise beam) or 57% (counterclockwise beam) for $p^\uparrow + p$, 58% for $p^\uparrow + \text{Al}$, and 61% for $p^\uparrow + \text{Au}$ collisions, with a relative uncertainty of 3% due to uncertainty in the polarization normalization. The beams are bunched. To minimize systematic effects due to time dependence of machine and detector performance, the spin configuration of the colliding bunches is alternated every 106 ns.

The PHENIX detector comprises two central arms at midrapidity and two muon arms at forward rapidity [52,53]; only reconstructed tracks from the muon arms are used for this analysis. The two muon spectrometers cover $1.2 < \eta < 2.4$ (polarized p -going direction) and $-2.2 < \eta < -1.2$ (A -going direction) in pseudorapidity with full azimuthal angle coverage. Each muon arm has 7.5 nuclear interaction lengths (λ_I) of hadron absorber followed by a muon tracker (MuTr), which is a set of three stations of cathode strip chambers for momentum measurements of charged particles. The MuTr determines the momentum of a charged particle in a radial magnetic field of $\int B dl = 0.72$ Tm with a momentum resolution of $\delta p/p \approx 0.05$ for hadrons in the kinematic range of this analysis. A muon identifier (MuID), located behind the MuTr, comprises five layers of stainless-steel absorbers ($\sim 5\lambda_I$ total) and Iarocci tube planes. The MuID helps to identify muons and hadrons based on the penetration depth of the tracks at $p_z \gtrsim 3.5$ GeV/ c [54].

The beam-beam counters (BBCs) [55], at $z = \pm 144$ cm from the nominal interaction point, comprise two arrays of

64 quartz Cherenkov detectors and cover the full azimuth and the pseudorapidity range $3.1 < |\eta| < 3.9$. The BBCs are used to determine the collision vertex z position ($|z| < 30$ cm cut was used in this analysis) as well as to provide a minimum-bias (MB) trigger with efficiencies of 55% for $p + p$, 72% for $p + \text{Al}$, and 84% for $p + \text{Au}$ collisions. The A -going side of the BBC is also used to determine the event centrality based on the distribution of the charge sum [56]. The recorded events are sampled by the MB trigger combined with muon triggers to enrich good muon and hadron tracks. The MuID provides a trigger for events containing one or more hadron or muon candidates. Momentum-sensitive triggering is provided by hit information from the MuTr to enrich tracks with $p_T > 3$ GeV/ c [57].

This analysis uses only charged tracks that stop in the middle of the MuID planes (third or fourth plane out of five planes) due to a hadronic interaction with the absorber material. In the kinematic region of $0.1 < x_F < 0.2$, where the longitudinal momentum of particles is larger than 10 GeV/ c , positively charged hadron candidates mostly comprise π^+ and K^+ .

The particle composition in the measured charged-hadron sample was estimated with a method developed in Refs. [54,58], based on identified charged-hadron spectra measured at midrapidity in $p + p$ and $d + \text{Au}$ collisions at RHIC [35,59,60], and extrapolated to PHENIX muon arm rapidity region of $1.2 < \eta < 2.4$ for $p + p$, $p + \text{Al}$ and $p + \text{Au}$ collisions using PYTHIA [61] and HIJING [62] event generators. The K^+/π^+ ratio of ~ 0.35 , as measured at RHIC at midrapidity at $p_T \sim 2$ GeV/ c (typical for our data) [35,59,60], was found approximately unchanged when extrapolated to forward rapidity in both $p + p$ and $p + A$ collisions. The p/π^+ ratio of ~ 0.25 (~ 0.35) at midrapidity in $p + p$ ($d + \text{Au}$) collisions [35,59,60] was extrapolated to the value of ~ 0.3 (~ 0.5) at the muon arm rapidity, with ratios in $p + \text{Al}$ and $p + \text{Au}$ collisions being in between values for $p + p$ and $d + \text{Au}$ collisions. The initial charged hadron composition is significantly modified due to particle interaction in the detector material, which according to Geant4-based [63] detector simulation modifies the initial K^+/π^+ (p/π^+) ratio by a factor of 2.7 (0.4), which varies by $\approx 5\%$ for different hadron interaction models [63]. As a result, the $\pi^+/K^+/p$ particle composition in our measured positively charged-hadron sample is evaluated to be 45%/47%/5% in $p + p$ collisions, with increased proton fraction to 7% (9%) in $p + \text{Al}$ ($p + \text{Au}$) collisions.

The unbinned maximum-likelihood method for extracting A_N was established in a previous study [64] that used the same detectors. Compared to binned approaches, this method is robust even for low-statistics data. The extended log-likelihood is defined to be

$$\log \mathcal{L} = \sum_i \log[1 + PA_N \sin(\phi_{\text{pol}} - \phi_h^i)] + \text{const}, \quad (1)$$

where ϕ_h^i is the azimuthal angle of the i th hadron with respect to the direction of the polarized proton beam, ϕ_{pol} is the azimuthal angle for the beam polarization direction, which in the 2015 PHENIX run takes the values $\pm (\pi/2)$ for \uparrow/\downarrow spin-signed beam bunches, respectively, and P is the beam polarization. The asymmetry A_N is determined by maximizing $\log \mathcal{L}$. For $p^\uparrow + p$ collisions, both beams are polarized; therefore the values of A_N were measured separately for each beam, found to be consistent, and were averaged in the final result. For $p^\uparrow + A$ collisions, only the clockwise proton beam was polarized. The statistical uncertainty was calculated from the second derivative of the log-likelihood estimator,

$$\sigma^2(A_N) = \left(-\frac{\partial^2 \mathcal{L}}{(\partial A_N)^2} \right)^{-1}. \quad (2)$$

The A_N calculated from the likelihood method is compared with the following azimuthal-fitting method based on the polarization formula [65]:

$$A_N(\phi) = \frac{\sigma^\uparrow(\phi) - \sigma^\downarrow(\phi)}{\sigma^\uparrow(\phi) + \sigma^\downarrow(\phi)} = \frac{1}{P} \frac{N^\uparrow(\phi) - RN^\downarrow(\phi)}{N^\uparrow(\phi) + RN^\downarrow(\phi)}, \quad (3)$$

where $A_N(\phi)$ is the simple count-based transverse single-spin asymmetry in each of the 16 azimuthal ϕ -bins, $\sigma^\uparrow, \sigma^\downarrow$ are cross sections for each polarization of spin up or down, N^\uparrow, N^\downarrow are yields, and $R = L^\uparrow/L^\downarrow$ is the luminosity ratio (relative luminosity) between bunches with spin up and down, determined from the number of sampled MB triggers corresponding to different spin orientations. From this, A_N is extracted from the fit of Eq. (3) with a function $A_N \sin(\phi_{\text{pol}\uparrow} - \phi)$, where $\phi_{\text{pol}\uparrow} = \pi/2$ is the azimuthal direction of the upward polarized bunches. Because every detector element is simultaneously used for the measurements with spin-up and -down, the possible systematic effects from acceptance nonuniformity and acceptance variation versus time are largely canceled. The relative variation between this method and the log likelihood method is included in the systematic uncertainty.

Figure 1 shows the reconstructed azimuthal modulation of positively charged hadrons for $0.1 < x_F < 0.2$ and $1.8 < p_T < 7.0$ GeV/c in $p^\uparrow + p$, $p^\uparrow + \text{Al}$, and $p^\uparrow + \text{Au}$ collisions at $\sqrt{s_{NN}} = 200$ GeV, as calculated using Eq. (3). The relatively larger statistical uncertainty in the bin at $\phi \sim 0.6$ rad is caused by a known detector inefficiency. The χ^2/NDF of the fits are 10.1/15 for $p^\uparrow + p$, 13.5/15 for $p^\uparrow + \text{Al}$, and 9.8/15 for $p^\uparrow + \text{Au}$. The $p^\uparrow + p$ results show a clear nonzero modulation, while the $p^\uparrow + \text{Al}$ results show a weaker modulation. In $p^\uparrow + \text{Au}$ collisions, the modulation is consistent with zero within the statistical uncertainty.

The finite momentum and azimuthal angle ϕ resolution in the MuTr and the interactions of particles with the materials prior to entering the MuTr lead to a kinematic

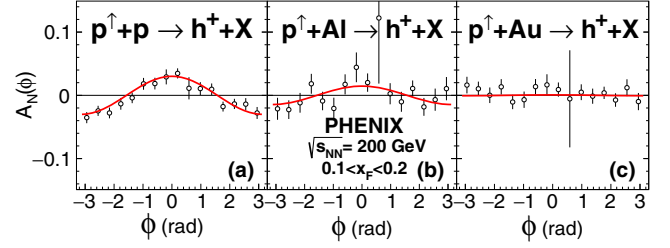


FIG. 1. Azimuthal modulation of positively charged hadrons for $1.4 < \eta < 2.4$, $0.1 < x_F < 0.2$, and $1.8 < p_T < 7.0$ GeV/c in (a) $p^\uparrow + p$, (b) $p^\uparrow + \text{Al}$, and (c) $p^\uparrow + \text{Au}$ collisions at $\sqrt{s_{NN}} = 200$ GeV.

smearing for the A_N measurement. This smearing effect was studied and corrected with a full detector Geant4 simulation. The effect due to the ϕ smearing was found to be negligible. The momentum smearing effect was evaluated by resolving a set of linear equations connecting A_N for the true x_F bins (A_N^{truth}) and A_N for the reconstructed x_F bins (A_N^{reco}):

$$A_N^{\text{reco},m} = \sum_i f^{i \rightarrow m} \cdot A_N^{\text{truth},i}, \quad (4)$$

where $A_N^{\text{reco},m}$ is A_N for the m -th reconstructed x_F bin from this measurement and $A_N^{\text{truth},i}$ is that for the i th true x_F bin. $f^{i \rightarrow m}$ represents the fraction of charged particles whose true x_F at the collision vertex belongs to the i th true x_F bin and is reconstructed as being in the m th x_F bin. $f^{i \rightarrow m}$ is obtained from the Geant4 detector simulation. For calculating A_N^{truth} by solving Eq. (4), the A_N^{reco} is measured in a wider x_F range $0.035 < x_F < 0.3$, by including two bins at lower x_F and one bin at higher x_F . The resulting smearing-corrected A_N^{truth} of the positively charged hadrons in bin $0.1 < x_F < 0.2$ are shown in Table I. The difference between the obtained A_N^{truth} and the measured A_N^{reco} is small compared to the statistical uncertainty and is accounted for in the systematic uncertainty.

Table I also summarizes the systematic uncertainties for the A_N measurements. The difference of A_N extracted with two methods, Eqs. (1) and (3), is shown as $\delta A_N^{\text{method}}$. The difference between the obtained A_N^{truth} and measured A_N^{reco}

TABLE I. A_N and sources of systematic uncertainty for positively charged hadrons for $1.4 < \eta < 2.4$, $0.1 < x_F < 0.2$, and $1.8 < p_T < 7.0$ GeV/c in $p^\uparrow + p$, $p^\uparrow + \text{Al}$, and $p^\uparrow + \text{Au}$ collisions at $\sqrt{s_{NN}} = 200$ GeV.

	$p^\uparrow + p$	$p^\uparrow + \text{Al}$	$p^\uparrow + \text{Au}$
A_N	3.14×10^{-2}	1.42×10^{-2}	0.12×10^{-2}
δA_N^{stat}	0.37×10^{-2}	0.72×10^{-2}	0.55×10^{-2}
δA_N^{syst}	$+0.05$ -0.18×10^{-2}	$+0.02$ -0.02×10^{-2}	$+0.06$ -0.06×10^{-2}
$\delta A_N^{\text{method}}$	$+0.05$ -0.05×10^{-2}	$+0.02$ -0.02×10^{-2}	$+0.06$ -0.06×10^{-2}
$\delta A_N^{\text{smear}}$	$+0.00$ -0.17×10^{-2}	$+0.01$ -0.00×10^{-2}	$+0.01$ -0.00×10^{-2}

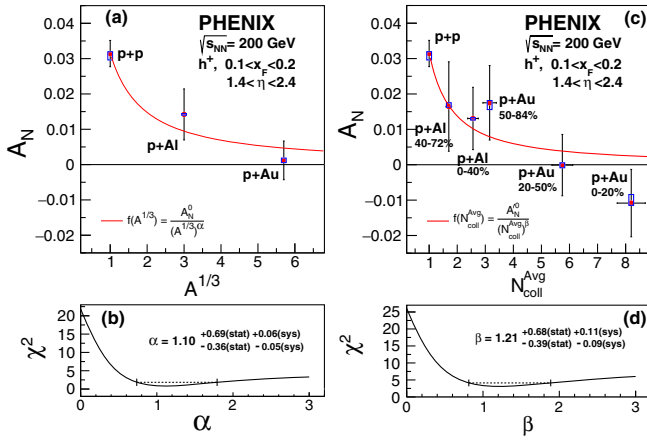


FIG. 2. Upper panels are A_N of positively charged hadrons for $0.1 < x_F < 0.2$, $1.8 < p_T < 7.0$ GeV/c, and $1.4 < \eta < 2.4$ in $p^\uparrow + p$, $p^\uparrow + Al$, and $p^\uparrow + Au$ collisions at $\sqrt{s_{NN}} = 200$ GeV as a function of (a) $A^{1/3}$ and (c) N_{coll}^{avg} . The fit functions, $A_N^0/(A^{1/3})^\alpha$ and $A_N^0/(N_{coll}^{avg})^\beta$ are shown as solid [red] curves. Vertical bars (boxes) represent statistical (systematic) uncertainties. A 3% scale uncertainty due to polarization uncertainty is not shown. Lower panels show χ^2 distributions as a function of power parameters (b) α and (d) β , taking into account the statistical uncertainty only. Dashed lines represent the range of α and β for $\Delta\chi^2 < 1$.

is assigned as a conservative systematic uncertainty due to the smearing effect, δA_N^{smear} . The total systematic uncertainty δA_N^{syst} is calculated as a quadratic sum of these two uncertainties.

Figure 2 shows A_N of positively charged hadrons in $p^\uparrow + p$, $p^\uparrow + Al$, and $p^\uparrow + Au$ collisions vs $A^{1/3}$ and the average number of nucleon-nucleon collisions N_{coll}^{avg} . The N_{coll}^{avg} is calculated using the Glauber model [66] for each centrality class in $p^\uparrow + A$ collisions [56]. The figure caption and legends denote the ranges of parameters and give the determined values of the power parameters α and β . Panels (b) and (d) show the χ^2 distributions with only statistical uncertainties included.

The recent efforts to calculate A_N in $p^\uparrow + p$ and $p^\uparrow + A$ collisions, accounting for gluon saturation effects [30, 49–51] suggested that A_N could be A independent or $A^{-1/3}$ dependent for the different contributions to A_N in the region where $p_T < Q_s$. However, $\langle p_T \rangle \sim 2.9$ GeV/c in our results is much larger than the saturation scale in the Au nucleus ($Q_s^{Au} \sim 0.9$ GeV) for the kinematics of this measurement and would lead to no strong A dependence of TSSAs under these models, as calculated in Ref. [51]. Nevertheless, the results in this Letter strongly disfavor the A -independent scenario.

The N_{coll}^{avg} dependence of A_N also suggests the decrease of A_N is related to the density of nuclear matter inside the target nucleus which the projectile proton traverses. This N_{coll}^{avg} dependence of A_N could be related to novel effects in

$p + A$ collisions, such as multiple scattering of partons in the initial and/or final stages of the hard scattering, which is also indicated in the recent results of the nuclear modification of single hadron production and transverse momentum broadening in dihadron correlations in $p + A$ collisions [35,67,68]. Another possibility is interaction of the parton with hot QCD matter produced in $p + A$ collisions, as suggested by recent results in small systems [36–38].

We note preliminary results from the STAR Collaboration [69] of measured A_N for π^0 in $p^\uparrow + p$ and $p^\uparrow + Au$ collisions in more forward kinematics at $2.6 < \eta < 4.0$, $0.2 < x_F < 0.7$, and $p_T > 1.5$ GeV/c that show small or no A dependence. The dramatic difference in A -dependence of TSSAs in different particle species and kinematic range emphasizes the importance of further detailed studies of A_N for different particle species over wide kinematics.

To summarize, we have reported A_N of positively charged hadrons for $1.4 < \eta < 2.4$, $0.1 < x_F < 0.2$, and $1.8 < p_T < 7.0$ GeV/c in $p^\uparrow + p$, $p^\uparrow + Al$, and $p^\uparrow + Au$ collisions at $\sqrt{s_{NN}} = 200$ GeV. For the first time, we observed an A dependent A_N in light hadron production in $p + A$ collisions, with the asymmetry values dropping from $\sim 3\%$ in $p + p$ collisions to a value consistent with zero in $p + Au$ collisions. These results may provide new insights into the origin of A_N and a unique tool to investigate the rich phenomena behind TSSAs in hadronic collisions and to use TSSAs as a new approach to studying the small-system collisions.

We thank the staff of the Collider-Accelerator and Physics Departments at Brookhaven National Laboratory and the staff of the other PHENIX participating institutions for their vital contributions. We also thank D. Pitonyak and M. Sievert for very useful discussions. We acknowledge support from the Office of Nuclear Physics in the Office of Science of the Department of Energy, the National Science Foundation, Abilene Christian University Research Council, Research Foundation of SUNY, and Dean of the College of Arts and Sciences, Vanderbilt University (U.S.A), Ministry of Education, Culture, Sports, Science, and Technology and the Japan Society for the Promotion of Science (Japan), Conselho Nacional de Desenvolvimento Científico e Tecnológico and Fundação de Amparo à Pesquisa do Estado de São Paulo (Brazil), Natural Science Foundation of China (People’s Republic of China), Croatian Science Foundation and Ministry of Science and Education (Croatia), Ministry of Education, Youth and Sports (Czech Republic), Centre National de la Recherche Scientifique, Commissariat à l’Énergie Atomique, and Institut National de Physique Nucléaire et de Physique des Particules (France), Bundesministerium für Bildung und Forschung, Deutscher Akademischer Austausch Dienst, and Alexander von Humboldt Stiftung (Germany), J. Bolyai Research Scholarship, EFOP, the

New National Excellence Program (ÚNKP), NKFIH, and OTKA (Hungary), Department of Atomic Energy and Department of Science and Technology (India), Israel Science Foundation (Israel), Basic Science Research and SRC(CENuM) Programs through NRF funded by the Ministry of Education and the Ministry of Science and ICT (Korea). Physics Department, Lahore University of Management Sciences (Pakistan), Ministry of Education and Science, Russian Academy of Sciences, Federal Agency of Atomic Energy (Russia), VR and Wallenberg Foundation (Sweden), the U.S. Civilian Research and Development Foundation for the Independent States of the Former Soviet Union, the Hungarian American Enterprise Scholarship Fund, the US-Hungarian Fulbright Foundation, and the US-Israel Binational Science Foundation.

*Deceased.

†PHENIX Spokesperson.

akiba@rcf.rhic.bnl.gov

- [1] R. D. Klem, J. E. Bowers, H. W. Courant, H. Kagan, M. L. Marshak, E. A. Peterson, K. Ruddick, W. H. Dragoset, and J. B. Roberts, Measurement of Asymmetries of Inclusive Pion Production in Proton Proton Interactions at 6 and 11.8 GeV/c, *Phys. Rev. Lett.* **36**, 929 (1976).
- [2] G. L. Kane, J. Pumplin, and W. Repko, Transverse Quark Polarization in Large p(T) Reactions, e^+e^- Jets, and Leptoproduction: A Test of QCD, *Phys. Rev. Lett.* **41**, 1689 (1978).
- [3] J. Antille, L. Dick, L. Madansky, D. Perret-Gallix, M. Werlen, A. Gonidec, K. Kuroda, and P. Kyberd, Spin dependence of the inclusive reaction $p + p$ (polarized) $\rightarrow \pi^0 + X$ at 24 GeV/c for high- p_T π^0 produced in the central region, *Phys. Lett. B* **94**, 523 (1980).
- [4] D. L. Adams *et al.* (FNAL-E704 Collaboration), Analyzing power in inclusive π^+ and π^- production at high x_F with a 200 GeV polarized proton beam, *Phys. Lett. B* **264**, 462 (1991).
- [5] D. L. Adams *et al.* (FNAL-E581 Collaboration), Comparison of spin asymmetries and cross sections in π^0 production by 200 GeV polarized antiprotons and protons, *Phys. Lett. B* **261**, 201 (1991).
- [6] C. E. Allgower *et al.* (AGS-E925 Collaboration), Measurement of analyzing powers of π^+ and π^- produced on a hydrogen and a carbon target with a 22-GeV/c incident polarized proton beam, *Phys. Rev. D* **65**, 092008 (2002).
- [7] J. Adams *et al.* (STAR Collaboration), Cross Sections and Transverse Single-Spin Asymmetries in Forward Neutral-Pion Production from Proton Collisions at $\sqrt{s} = 200$ GeV, *Phys. Rev. Lett.* **92**, 171801 (2004).
- [8] J. H. Lee and F. Videbaek (BRAHMS Collaboration), Single-spin asymmetries of identified hadrons in polarized $p + p$ at $\sqrt{s} = 62.4$ and 200 GeV, *AIP Conf. Proc.* **915**, 533 (2007).
- [9] B. I. Abelev *et al.* (STAR Collaboration), Forward Neutral-Pion Transverse Single-Spin Asymmetries in $p + p$ Collisions at $\sqrt{s} = 200$ GeV, *Phys. Rev. Lett.* **101**, 222001 (2008).
- [10] I. Arsene *et al.* (BRAHMS Collaboration), Single Transverse Spin Asymmetries of Identified Charged Hadrons in Polarized $p + p$ Collisions at $\sqrt{s} = 62.4$ GeV, *Phys. Rev. Lett.* **101**, 042001 (2008).
- [11] L. Adamczyk *et al.* (STAR Collaboration), Transverse single-spin asymmetry and cross-section for π^0 and η mesons at large feynman- x in polarized $p + p$ collisions at $\sqrt{s} = 200$ GeV, *Phys. Rev. D* **86**, 051101 (2012).
- [12] A. Adare *et al.* (PHENIX Collaboration), Measurement of transverse-single-spin asymmetries for midrapidity and forward-rapidity production of hadrons in polarized $p + p$ collisions at $\sqrt{s} = 200$ and 62.4 GeV, *Phys. Rev. D* **90**, 012006 (2014).
- [13] A. Adare *et al.* (PHENIX Collaboration), Cross section and transverse single-spin asymmetry of η mesons in $p^\uparrow + p$ collisions at $\sqrt{s} = 200$ GeV at forward rapidity, *Phys. Rev. D* **90**, 072008 (2014).
- [14] M. M. Mondal (STAR Collaboration), Measurement of the transverse single-spin asymmetries for π^0 and jet-like events at forward rapidities at STAR in $p + p$ collisions at $\sqrt{s} = 500$ GeV, *Proc. Sci.*, DIS2014 (2014) 216.
- [15] D. W. Sivers, Single-spin production asymmetries from the hard scattering of point-like constituents, *Phys. Rev. D* **41**, 83 (1990).
- [16] D. W. Sivers, Hard scattering scaling laws for single-spin production asymmetries, *Phys. Rev. D* **43**, 261 (1991).
- [17] J. C. Collins, Fragmentation of transversely polarized quarks probed in transverse momentum distributions, *Nucl. Phys. B* **396**, 161 (1993).
- [18] A. Efremov and O. Teryaev, On spin effects in quantum chromodynamics, *Yad. Fiz.* **36**, 242 (1982) [*Sov. J. Nucl. Phys.* **36**, 140 (1982)].
- [19] J.-W. Qiu and G. F. Sterman, Single transverse spin asymmetries in hadronic pion production, *Phys. Rev. D* **59**, 014004 (1998).
- [20] C. Kouvaris, J.-W. Qiu, W. Vogelsang, and F. Yuan, Single transverse-spin asymmetry in high transverse momentum pion production in pp collisions, *Phys. Rev. D* **74**, 114013 (2006).
- [21] Y. Koike and K. Tanaka, Universal structure of twist-3 soft-gluon-pole cross-sections for single transverse-spin asymmetry, *Phys. Rev. D* **76**, 011502(R) (2007).
- [22] Y. Koike and T. Tomita, Soft-fermion-pole contribution to single-spin asymmetry for pion production in pp collisions, *Phys. Lett. B* **675**, 181 (2009).
- [23] K. Kanazawa and Y. Koike, New analysis of the single transverse-spin asymmetry for Hadron production at RHIC, *Phys. Rev. D* **82**, 034009 (2010).
- [24] Z.-B. Kang, J.-W. Qiu, W. Vogelsang, and F. Yuan, An observation concerning the process dependence of the Sivers functions, *Phys. Rev. D* **83**, 094001 (2011).
- [25] K. Kanazawa and Y. Koike, A phenomenological study on single transverse-spin asymmetry for inclusive light-hadron productions at RHIC, *Phys. Rev. D* **83**, 114024 (2011).
- [26] Z.-B. Kang and A. Prokudin, Global fitting of single-spin asymmetry: An attempt, *Phys. Rev. D* **85**, 074008 (2012).
- [27] H. Beppu, K. Kanazawa, Y. Koike, and S. Yoshida, Three-gluon contribution to the single-spin asymmetry for light

- hadron production in pp collision, *Phys. Rev. D* **89**, 034029 (2014).
- [28] A. Metz and D. Pitonyak, Fragmentation contribution to the transverse single-spin asymmetry in proton-proton collisions, *Phys. Lett. B* **723**, 365 (2013); Erratum *Phys. Lett. B* **762**, 549(E) (2016).
- [29] K. Kanazawa, Y. Koike, A. Metz, and D. Pitonyak, Towards an explanation of transverse single-spin asymmetries in proton-proton collisions: The role of fragmentation in collinear factorization, *Phys. Rev. D* **89**, 111501(R) (2014).
- [30] L. Gamberg, Z.-B. Kang, D. Pitonyak, and A. Prokudin, Phenomenological constraints on A_N in $p^\dagger p \rightarrow \pi X$ from Lorentz invariance relations, *Phys. Lett. B* **770**, 242 (2017).
- [31] I. Alekseev *et al.*, Polarized proton collider at RHIC, *Nucl. Instrum. Methods Phys. Res., Sect. A* **499**, 392 (2003).
- [32] J. W. Cronin, H. J. Frisch, M. J. Shochet, J. P. Boymond, R. Mermod, P. A. Piroue, and R. L. Sumner, Production of hadrons with large transverse momentum at 200, 300, and 400 GeV, *Phys. Rev. D* **11**, 3105 (1975).
- [33] S. S. Adler *et al.* (PHENIX Collaboration), Absence of Suppression in Particle Production at Large Transverse Momentum in $\sqrt{s_{NN}} = 200$ GeV $d + Au$ Collisions, *Phys. Rev. Lett.* **91**, 072303 (2003).
- [34] G. Aad *et al.* (ATLAS Collaboration), Transverse momentum, rapidity, and centrality dependence of inclusive charged-particle production in $\sqrt{s_{NN}} = 5.02$ TeV $p + Pb$ collisions measured by the ATLAS experiment, *Phys. Lett. B* **763**, 313 (2016).
- [35] A. Adare *et al.* (PHENIX Collaboration), Spectra and ratios of identified particles in Au + Au and $d + Au$ collisions at $\sqrt{s_{NN}} = 200$ GeV, *Phys. Rev. C* **88**, 024906 (2013).
- [36] K. Dusling, W. Li, and B. Schenke, Novel collective phenomena in high-energy proton-proton and proton-nucleus collisions, *Int. J. Mod. Phys. E* **25**, 1630002 (2016).
- [37] J. L. Nagle and W. A. Zajc, Small system collectivity in relativistic hadronic and nuclear collisions, *Annu. Rev. Nucl. Part. Sci.* **68**, 211 (2018).
- [38] C. Aidala *et al.* (PHENIX Collaboration), Creating small circular, elliptical, and triangular droplets of quark-gluon plasma, *Nat. Phys.* **15**, 214 (2019).
- [39] F. Gelis, E. Iancu, J. Jalilian-Marian, and R. Venugopalan, The color glass condensate, *Annu. Rev. Nucl. Part. Sci.* **60**, 463 (2010).
- [40] A. Schäfer and J. Zhou, Transverse single-spin asymmetry in direct photon production in polarized pA collisions, *Phys. Rev. D* **90**, 034016 (2014).
- [41] J. Zhou, Transverse single-spin asymmetry in Drell-Yan production in polarized pA collisions, *Phys. Rev. D* **92**, 014034 (2015).
- [42] D. Boer, A. Dumitru, and A. Hayashigaki, Single transverse-spin asymmetries in forward pion production at high energy: Incorporating small- x effects in the target, *Phys. Rev. D* **74**, 074018 (2006).
- [43] Z.-B. Kang and F. Yuan, Single-spin asymmetry scaling in the forward rapidity region at RHIC, *Phys. Rev. D* **84**, 034019 (2011).
- [44] Y. V. Kovchegov and M. D. Sievert, A new mechanism for generating a single transverse spin asymmetry, *Phys. Rev. D* **86**, 034028 (2012); Erratum *Phys. Rev. D* **86**, 079906(E) (2012).
- [45] Z.-B. Kang and B.-W. Xiao, Sivers asymmetry of Drell-Yan production in small- x regime, *Phys. Rev. D* **87**, 034038 (2013).
- [46] J. Zhou, Transverse single-spin asymmetries at small x and the anomalous magnetic moment, *Phys. Rev. D* **89**, 074050 (2014).
- [47] T. Altinoluk, N. Armesto, G. Beuf, M. Martínez, and C. A. Salgado, Next-to-eikonal corrections in the CGC: Gluon production and spin asymmetries in pA collisions, *J. High Energy Phys.* **07** (2014) 068.
- [48] D. Boer, M. G. Echevarria, P. J. Mulders, and J. Zhou, Single-Spin Asymmetries from a Single Wilson Loop, *Phys. Rev. Lett.* **116**, 122001 (2016).
- [49] Y. Hatta, B.-W. Xiao, S. Yoshida, and F. Yuan, Single-spin asymmetry in forward pA collisions, *Phys. Rev. D* **94**, 054013 (2016).
- [50] Y. Hatta, B.-W. Xiao, S. Yoshida, and F. Yuan, Single-spin asymmetry in forward pA collisions II: Fragmentation contribution, *Phys. Rev. D* **95**, 014008 (2017).
- [51] S. Benić and Y. Hatta, Single spin asymmetry in forward pA collisions: Phenomenology at RHIC, *Phys. Rev. D* **99**, 094012 (2019).
- [52] K. Adcox *et al.* (PHENIX Collaboration), PHENIX detector overview, *Nucl. Instrum. Methods Phys. Res., Sect. A* **499**, 469 (2003).
- [53] H. Akikawa *et al.* (PHENIX Collaboration), PHENIX muon arms, *Nucl. Instrum. Methods Phys. Res., Sect. A* **499**, 537 (2003).
- [54] A. Adare *et al.* (PHENIX Collaboration), Nuclear-modification factor for open-heavy-flavor production at forward rapidity in Cu + Cu collisions at $\sqrt{s_{NN}} = 200$ GeV, *Phys. Rev. C* **86**, 024909 (2012).
- [55] M. Allen *et al.* (PHENIX Collaboration), PHENIX inner detectors, *Nucl. Instrum. Methods Phys. Res., Sect. A* **499**, 549 (2003).
- [56] A. Adare *et al.* (PHENIX Collaboration), Centrality categorization for $R_{p(d)+A}$ in high-energy collisions, *Phys. Rev. C* **90**, 034902 (2014).
- [57] S. Adachi *et al.*, Trigger electronics upgrade of PHENIX muon tracker, *Nucl. Instrum. Methods Phys. Res., Sect. A* **703**, 114 (2013).
- [58] A. Adare *et al.* (PHENIX Collaboration), Cold-Nuclear-Matter Effects on Heavy-Quark Production at Forward and Backward Rapidity in $d + Au$ Collisions at $\sqrt{s_{NN}} = 200$ GeV, *Phys. Rev. Lett.* **112**, 252301 (2014).
- [59] A. Adare *et al.* (PHENIX Collaboration), Identified charged hadron production in $p + p$ collisions at $\sqrt{s} = 200$ and 62.4 GeV, *Phys. Rev. C* **83**, 064903 (2011).
- [60] G. Agakishiev *et al.* (STAR Collaboration), Identified Hadron Compositions in $p + p$ and Au + Au Collisions at High Transverse Momenta at $\sqrt{s_{NN}} = 200$ GeV, *Phys. Rev. Lett.* **108**, 072302 (2012).
- [61] T. Sjöstrand, S. Mrenna, and P. Z. Skands, PYTHIA 6.4 physics and manual, *J. High Energy Phys.* **05** (2006) 026.
- [62] M. Gyulassy and X.-N. Wang, HIJING 1.0: A Monte Carlo program for parton and particle production in high-energy hadronic and nuclear collisions, *Comput. Phys. Commun.* **83**, 307 (1994).
- [63] J. Allison *et al.*, Recent developments in Geant4, *Nucl. Instrum. Methods Phys. Res., Sect. A* **835**, 186 (2016).

- [64] C. Aidala *et al.* (PHENIX Collaboration), Cross section and transverse single-spin asymmetry of muons from open heavy-flavor decays in polarized $p + p$ collisions at $\sqrt{s} = 200$ GeV, *Phys. Rev. D* **95**, 112001 (2017).
- [65] G. G. Ohlsen and P. W. Keaton, Techniques for measurement of spin-1/2 and spin-1 polarization analyzing tensors, *Nucl. Instrum. Methods* **109**, 41 (1973).
- [66] M. L. Miller, K. Reygers, S. J. Sanders, and P. Steinberg, Glauber modeling in high energy nuclear collisions, *Annu. Rev. Nucl. Part. Sci.* **57**, 205 (2007).
- [67] C. Aidala *et al.* (PHENIX Collaboration), Nonperturbative transverse momentum broadening in dihadron angular correlations in $\sqrt{s_{NN}} = 200$ GeV proton-nucleus collisions, *Phys. Rev. C* **99**, 044912 (2019).
- [68] C. Aidala *et al.* (PHENIX Collaboration), Nuclear-modification factor of charged hadrons at forward and backward rapidity in $p + \text{Al}$ and $p + \text{Au}$ collisions at $\sqrt{s_{NN}} = 200$ GeV, [arXiv:1906.09928](https://arxiv.org/abs/1906.09928).
- [69] S. Heppelmann (STAR Collaboration), Preview from RHIC Run 15 pp and p Au forward neutral pion production from transversely polarized protons, in *Proceedings, 7th International Workshop on Multiple Partonic Interactions at the LHC (MPI@LHC 2015)* (2016), p. 228, <http://indico.ictp.it/event/a14280/>.